Secondary restoration control of islanded microgrids with a decentralized event-triggered strategy

Chen, Meng; Xiao, Xiangning ; Guerrero, Josep M.

Published in:
I E E E Transactions on Industrial Informatics

DOI (link to publication from Publisher):
10.1109/TII.2017.2784561

Publication date:
2018

Document Version
Accepted author manuscript, peer reviewed version

This article has been accepted for publication in a future issue of this journal, but has not been fully edited. Content may change prior to final publication. Citation information: DOI 10.1109/TII.2017.2784561, IEEE Transactions on Industrial Informatics

Secondary Restoration Control of Islanded Microgrids With Decentralized Event-triggered Strategy

Meng Chen, Xiangning Xiao, and Josep M. Guerrero, *Fellow, IEEE*

***Abstract*—Distributed cooperative control methods attract more and more attention in microgrid secondary control because they are more reliable and flexible. However, the traditional methods rely on the periodic communication, which is neither economic nor efficient due to its large communication burden. In this paper, an event-triggered approach based distributed control strategy is used to deal with the secondary frequency and voltage control in the islanded microgrid. By using the outputs of estimators, which are reset to the actual values only at the event-triggered time, to replace the actual values in the feedback control laws, the proposed control strategies just require the communication between distributed secondary controllers at some particular instants while having frequency and voltage restoration function and accurate active power sharing. The stability and inter-event interval are also analyzed in this paper. An islanded microgrid test system is built in PSCAD/EMTDC to validate the proposed control strategies. It shows that the proposed secondary control strategies based on event-triggered approach can highly reduce the inter-agent communication.**

***Index Terms*--Distributed control, microgrid, secondary control, event-triggered strategy, power sharing, inter-event interval.**

NOMENCLATURE

ω_i, ω_{ni}	Output frequency and its set-value of DG*i*.
V_i, V_{ni}	Voltage amplitude and its set-value of DG*i*.
D_{pi}, D_{qi}	Frequency and voltage droop coefficients.
p_i, P_i	Output and filtered active power of DG*i*.
q_i, Q_i	Output and filtered reactive power of DG*i*.
ω_c	Cut-off frequency of low-pass filter.
v_{di}, v_{qi}	Output voltages in the *d-q* coordinate of DG*i*.
i_{odi}, i_{oqi}	Output currents in the *d-q* coordinate of DG*i*.
$u_{\omega i}$, u_{pi}, u_{vi}	Frequency, active power and voltage control inputs of DG*i*.
$y_{\omega i}$, y_{pi}, y_{vi}	Frequency, active power and voltage control outputs of DG*i*.
$e_{\omega i}$, e_{pi}, e_{vi}	Frequency, active power and voltage local neighborhood tracking error of DG*i*.
d_i	Pinning gain of DG*i*.
$\eta_{\omega i}$, η_{vi}	Frequency, active power and voltage local disagreement.
$t_k^{\omega i}$ t_k^{pi} t_k^{vi}	Event-triggered time of the frequency, active power and voltage control for agent*i*.
$f_{\omega i}$, f_{pi}, f_{vi}	Triggering functions of the frequency, active power and voltage control for the agent*i*.

This work was supported by the Fundamental Research Funds of the Central Universities under Grant 2016XS01.

M. Chen and X. Xiao are with the State Key Laboratory for Alternate Electrical Power System with Renewable Energy Source, North China Electric Power University, Beijing, 102206 China (e-mail: chen_free@ ncepu.edu.cn; xxn@ncepu.edu.cn).

J. M. Guerrero is with the Institute of Energy Technology, Aalborg University, Aalborg, 9220 Denmark (e-mail: joz@et.aau.dk).

I. INTRODUCTION

THE microgrids have been proved as an effective and efficient way to integrate and manage distributed generations (DGs)[1] [2]. To keep the stable operation under islanded mode, a hierarchical structure of microgrids control, which is organized in three levels, is proposed in [3] and [4]. The primary control level follows the *P-ω* and *Q-V* droops, or some improved forms, to stabilize voltage and frequency by deviating them from the reference values. Then the secondary control level is necessary to compensate these deviations. Finally, the tertiary level determines set-points of secondary level to regulate power of system and optimize operation. This paper focus on the secondary level control. When considering the power regulation, it is in the scope of tertiary level. Research on tertiary level can be found in [4], [6] and [33].

Traditionally, the secondary level is designed in centralized way, that is, the microgrid central controller (MGCC) monitors the voltage and frequency of the system, generates set-points using a PI controller and send them to all the primary controllers via a star communication network [5]. This kind of communication structure is neither economic nor reliable [6].

Recently, in order to develop more reliable and autonomous control structures, the distributed cooperative control is introduced to solve the secondary restoration control for an islanded microgrid. In [7] and [8], the secondary control of islanded microgrids is transferred to the tracking synchronization problem of the multi-agent systems (MAS) using feedback linearization. In this context, DGs in the microgrid are considered as agents in the MAS. Then both voltage and frequency can be restored to their reference values with accurate real power sharing by communications between neighboring agents, although only a small portion of DGs can directly access to the leader. Actually, in an islanded microgrid,

This article has been accepted for publication in a future issue of this journal, but has not been fully edited. Content may change prior to final publication. Citation information: DOI 10.1109/TII.2017.2784561, IEEE Transactions on Industrial Informatics

there is inherently coupling between active and reactive power which means voltage and frequency will influence each other. To solve this problems, [9] proposes a distributed finite-time control method to address voltage restoration. Then design of the secondary voltage and frequency control can be separate. Similarly, the distributed finite-time control protocol can also be used to deal with the frequency restoration while having active power sharing based on their ratings [10]. Besides, distributed control has also been reported to deal with secondary control of the virtual synchronous generator [11]. In addition, optimal power routing problem among DC microgrid clusters is discussed using communication method in [35]. It should be noted that, all methods above are based on periodic sampled-data control which implies high communication burden between agents. In practice, the bandwidth of the communication network is limited, and therefore, it is necessary to reduce the communication burden to make the communication network more efficient and effective [12]. A discrete-time control was proposed in [13] to design the secondary control for islanded microgrids. However, the updating period is fixed, and therefore there is still much unnecessary communication though the communication burden is reduced comparing with those in [7]-[11].

Most recently, the event-triggered communication way is proposed in MAS. This kind of approach is implanted in a aperiodic fashion in contrast to the commonly periodic way. Therefore, it can reduce the communication burden among the sensors, controllers and actuators as well as improving the efficiency of the whole system [30].

In the last several years, the event-triggered control has been used in microgrid control to reduce information exchange between DGs. Both centralized and distributed power controllers have been proposed in [14] using the event-triggered communication. In [31], optimization is taken into consideration to reduce the event sampling. However, the controllers are not droop-based so that the system cannot operate in case of communication failure [12]. To solve this, a droop-based distributed reactive power sharing control for microgrids with event-triggered communication is proposed in [12]. Besides, the similar idea is also used in DC microgrid to achieve current sharing and eliminate voltage drops [15]. To the authors' knowledge, the secondary voltage and frequency restoration control using the event-triggered communication for an islanded AC microgrid has not been discussed.

In this paper, we focus on the distributed secondary voltage and frequency restoration control by taking into account the communication burden. The communication approach of distributed controllers is changed from the traditional periodic sampling way into a new event-triggered aperiodic sampling way. Triggering functions are designed to determine the event-triggered instants for all the voltage, frequency and active power controllers. By conducting the stability analysis, it shows that the proposed control scheme satisfies the Lyapunov stability, which means that all the output voltages and frequencies of DGs can synchronize to the reference values while maintaining the active power sharing according to their ratings. Different simulation results have validated the effectiveness of the proposed event-triggered approach.

The main contributions of the paper are summarized as:

1) Both output voltages of DGs and frequency of the islanded microgrid are restored to their reference values while keeping active power sharing accuracy using distributed event-triggered control. Thus communication burden between agents is highly reduced than that the periodic communication way.
2) To define the event-triggered condition and sampling, a new distributed event-triggering rule is proposed for all the controllers of frequency, voltage and active power, to construct the secondary control level, which is easy to follow.
3) The stability of the proposed control strategy is proved using Lyapunov method. And the lower bound of the inter-event interval is also discussed to prevent infinite event-triggered instants in a finite time period.

The rest of this paper is organized as follows. In Section II, the local primary control of DGs is introduced. The secondary voltage and frequency controls based on decentralized event-triggered control of the islanded microgrids are presented in Section III. The triggering function and sampling are also included in Section III. Section IV proves the stability of the proposed control strategy and discusses the lower bound of the inter-event interval. The proposed secondary control is validated in Section V through simulations in PSCAD/EMTDC. Section VI concludes this paper.

II. Primary Control Of Islanded Microgrids

The schematic view of the proposed control strategy can be illustrated in Fig. 1. Usually, DGs are connected to the microgrid through power electronics inverters and the power stage of the DGs also includes an LC filter and a line. The primary control scheme implemented in *d-q* coordinates includes four different parts which are power calculation block, droop controller, voltage and current controllers, and PWM modulator [16]. The secondary control provides set-points for the primary control. As seen, not only local information is needed but also neighboring information is delivered to the secondary controller by communication link. In comparison to the traditional periodic communication way, the method in this paper is event-triggered.

The droop controller mimics the droop mechanism of the traditional synchronous generator to regulate ω_i and V_i according to active and reactive power respectively, and can be expressed as [17], [18]

$$\omega_i = \omega_{ni} - D_{pi} P_i \quad (1)$$

$$V_i = V_{ni} - D_{qi} Q_i \quad (2)$$

where ω_i and V_{ni} are derived by the secondary control level. The primary control makes DGs share the active and reactive power autonomously. Meanwhile, in this case, the droop characteristics make voltage and frequency of the microgrid deviate from the rated values. Usually, P_i and Q_i in (1) and (2)

This article has been accepted for publication in a future issue of this journal, but has not been fully edited. Content may change prior to final publication. Citation information: DOI 10.1109/TII.2017.2784561, IEEE Transactions on Industrial Informatics

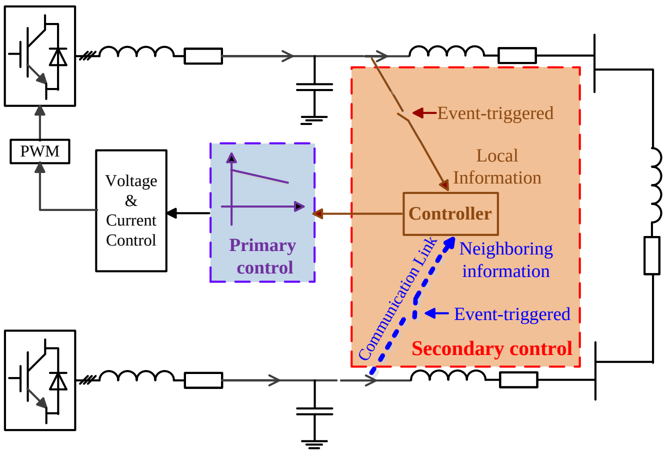

Fig. 1. Schematic view of the proposed control structure.

can be obtained via two first-order low-pass filters (LPF) as the following [19]

$$P_i = \frac{\omega_c}{s+\omega_c} p_i \tag{3}$$

$$Q_i = \frac{\omega_c}{s+\omega_c} q_i \tag{4}$$

where p_i and q_i are calculated by the power calculation block which can be expressed as [20]

$$p_i = v_{di} i_{odi} + v_{qi} i_{oqi} \tag{5}$$

$$q_i = v_{qi} i_{odi} - v_{di} i_{oqi} \tag{6}$$

III. Secondary Control of Islanded Microgrids

In an islanded microgrid, the frequency is same globally in the steady-state. However, the output voltages of DGs may be different [32]. In this paper, we use the decentralized event-triggered secondary control to restore the output voltages of all DGs. Furthermore, the frequency restoration with accurate active power sharing is also handled. The control objectives can be expressed as follows.

1) Frequency restoration with accurate active power sharing, i.e.,

$$\lim_{t\to\infty} \omega_i(t) = \omega_{ref},\ \forall i \tag{7}$$

$$\lim_{t\to\infty}[D_{pi}P_i(t)] = \lim_{t\to\infty}[D_{pj}P_j(t)],\ \forall i,\ j \tag{8}$$

2) Output voltages restoration of all DGs, i.e.,

$$\lim_{t\to\infty} V_i(t) = V_{ref},\ \forall i \tag{9}$$

A. Graph Theory

An islanded microgrid can be seen as a MAS if considering DGs as agents. In this section, the basic knowledge of graph theory is firstly introduced for convenience to describe the communication network of the MAS, which can be modelled by a graph.

A graph is expressed by a triple G=(V(G), E(G), $\boldsymbol{A_G}$) consisting of a nonempty finite set of N vertex, i.e. agents, $V(G)=\{v_1, v_2, \ldots, v_N\}$, a set of edges, i.e. links between agents, $E(G)\subset V(G)\times V(G)$, and the adjacency matrix $\boldsymbol{A_G}\subset R^{N\times N}$. $(v_j, v_i)\subset E(G)$ denotes an edge which means the ith agent can receive information from the jth agent. The graph G is said to be undirected if for all edges $(v_j, v_i)\subset E(G)$, $(v_i, v_j)\subset E(G)$. The set of neighbors of the ith agent is defined as $N_i=\{v_j\in V(G)|(v_j, v_i)\subset E(G),\ i\neq j\}$. The elements of $\boldsymbol{A_G}$ are defined as $a_{ij}=1$ if $v_j\in N_i$, otherwise $a_{ij}=0$. The degree matrix $\boldsymbol{\Delta}$ is defined as $\boldsymbol{\Delta}=\mathrm{diag}\{\Delta_i\}$ with $\Delta_i=\sum_{v_j\in N_i} a_{ij}$. The Laplacian matrix $\boldsymbol{L}$ is defined as $\boldsymbol{L}=\boldsymbol{\Delta}-\boldsymbol{A_G}$. A sequence of edges $\{(v_i, v_k), (v_k, v_l), \ldots, (v_s, v_j)\}$ is a path from agent$i$ to agent$j$. If there exists a path from all $v_i\in V(G)$ to all $v_j\in V(G)$, the undirected graph is said to be connected [21], [22]. In addition, in the following, the communication network of the islanded microgrid is also denoted as G for convenience.

B. Distributed Secondary Controller Design

The distributed control scheme of an islanded microgrid can be illustrated in Fig. 2. In this scheme, references are only known to a few agents. The secondary control objectives are achieved locally with a communication network rather than relying on a central controller. A virtual agent denoting as agent0 provides the references for secondary controllers. Then agent0 can be considered as a leader node and all the other agents synchronize to it. Furthermore, the active power sharing can be seen as a leaderless consensus problem. In this way, control objectives in (7)-(9) can be achieved.

1) Frequency restoration: The dynamics of the primary control are dominated by the droop control in (1) and (2) [19].

Therefore, fast dynamics can be neglected when designing the secondary control level [5] [7]. Constructing the state-space model of the frequency control as the following

$$\begin{cases}\dot{\omega}_i(t) = u_{\omega i}(t)\\ y_{\omega i}(t) = \omega_i(t)\end{cases} \tag{10}$$

Traditionally, to solve the leader-followers consensus, a distributed controller can be constructed as [23]

$$u_{\omega i}(t) = k_\omega e_{\omega i}(t) \tag{11}$$

where $k_\omega>0$ and $e_{\omega i}(t)$ is defined as

$$e_{\omega i}(t) = \sum_{j\in N_i}[\omega_j(t)-\omega_i(t)] + d_i[\omega_{ref}-\omega_i(t)] \tag{12}$$

where d_i is nonzero for the agent that can receive the references from agent0. As seen from (11) and (12), this kind of distributed controllers rely on continuous states feedback which implies high communication burden between agents. Then the requirement to the communication network is relatively high. In this paper, a decentralized event-triggered control strategy, see e.g., [24], [25], [26], is presented to reduce inter-agent communication while ensuring the system asymptotically stable.

In the proposed distributed control law, (12) is redefined as following in (13)

This article has been accepted for publication in a future issue of this journal, but has not been fully edited. Content may change prior to final publication. Citation information: DOI 10.1109/TII.2017.2784561, IEEE Transactions on Industrial Informatics

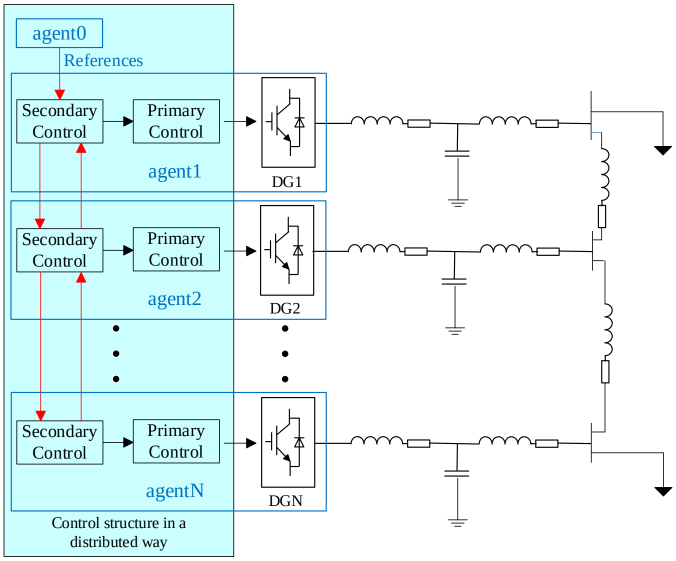

Fig. 2. Distributed control scheme of islanded microgrids.

$$e_{\omega i}(t)=\sum_{j\in N_i}[\hat{\omega}_j(t)-\hat{\omega}_i(t)]+d_i[\omega_{ref}-\hat{\omega}_i(t)] \tag{13}$$

where the superscript ∧ means the estimates of the corresponding variables which are defines as

$$\hat{\omega}_i(t)=\omega_i(t_k^{\omega i}),\ t\in[t_k^{\omega i},\ t_{k+1}^{\omega i}) \tag{14}$$

Defining $\eta_{\omega i}(t)$ and the estimate error $\varepsilon_{\omega i}(t)$, respectively, as

$$\eta_{\omega i}(t)=\omega_i(t)-\omega_{ref} \tag{15}$$

$$\varepsilon_{\omega i}(t)=\omega_i(t_k^{\omega i})-\omega_i(t) \tag{16}$$

Then the generation of event-triggered time can be illustrated by Fig. 3. When $\|\varepsilon_{\omega i}(t)\|$ reaches an upper bound, the event is triggered with $\|\varepsilon_{\omega i}(t)\|$ being updated to zero for the state estimate equaling to the actual value due to communication. Then $\|\varepsilon_{\omega i}(t)\|$ increases until the next event-triggered time comes. As a result, $\|\varepsilon_{\omega i}(t)\|$ can be convergent to zero. During the intervals between the event-triggered times, no communication is needed. The upper bound can be determined by the triggering function. In this paper, every DG has its own triggering function which is defined using only local and neighbors' information. Thus a whole distributed scheme can be built.

Theorem 1**:** Let G be connected and at least one agent can receive information from the leader node. Then the distributed controllers in (11) and (13) ensures global stability of the frequency dynamics system if the event-triggered time is defined by the following

$$t_k^{\omega i}=\inf\{t>t_{k-1}^{\omega i}\mid f_{\omega i}(t)=0\} \tag{17}$$

where $f_{\omega i}(t)$ can be defined as

$$f_{\omega i}(t)=\|\varepsilon_{\omega i}(t)\|^2-\frac{\alpha_\omega(1-\beta_\omega\sum_{j\in N_i}a_{ij}-\beta_\omega d_i/2)}{\sum_{j\in N_i}a_{ij}/\beta_\omega+d_i/(2\beta_\omega)}\|e_{\omega i}(t)\|^2 \tag{18}$$

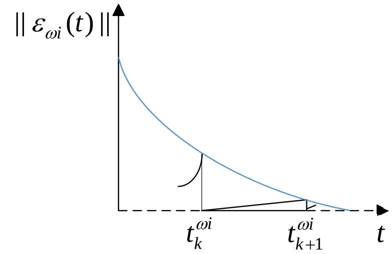

Fig. 3. Event-triggered time generation mechanism.

where $0<\alpha_\omega<1$. Furthermore, there is

$$0<\beta_\omega<\frac{1}{\sum_{j\in N_i}a_{ij}+d_i/2},\ \forall i \tag{19}$$

For active power sharing, the state-space model can be constructed as

$$\begin{cases}D_{pi}\dot{P}_i(t)=u_{pi}(t)\\ y_{pi}(t)=D_{pi}P_i(t)\end{cases} \tag{20}$$

Constructing the distributed controller as

$$u_{pi}(t)=k_p e_{pi}(t) \tag{21}$$

where $k_p>0$ and $e_{pi}(t)$ is defined as

$$e_{pi}(t)=\sum_{j\in N_i}[D_{pj}\hat{P}_j(t)-D_{pi}\hat{P}_i(t)] \tag{22}$$

where definition of the estimate is similar with that in (14). Then defining the active power estimate error as

$$\varepsilon_{pi}(t)=D_{pi}P_i(t_k^{pi})-D_{pi}P_i(t) \tag{23}$$

Theorem 2**:** Let G be connected. Then the distributed controllers in (21) and (22) ensures global stability of the active power dynamics system if the event-triggered time is defined by the following

$$t_k^{pi}=\inf\{t>t_{k-1}^{pi}\mid f_{pi}(t)=0\} \tag{24}$$

where $f_{pi}(t)$ can be defined as

$$f_{pi}(t)=\|\varepsilon_{pi}(t)\|^2-\frac{\alpha_p(1-\beta_p\sum_{j\in N_i}a_{ij})}{\sum_{j\in N_i}a_{ij}/\beta_p}\|e_{pi}(t)\|^2 \tag{25}$$

where $0<\alpha_p<1$. Furthermore, there is

$$0<\beta_\omega<1/\sum_{j\in N_i}a_{ij},\ \forall i \tag{26}$$

Then combining (1), (10) and (20), the set-value of the frequency primary control can be derived as

$$\omega_{ni}(t)=\int[u_{\omega i}(t)+u_{pi}(t)]dt \tag{27}$$

2) Voltage restoration: Similar to (10), constructing the state-space model of the voltage control as the following

This article has been accepted for publication in a future issue of this journal, but has not been fully edited. Content may change prior to final publication. Citation information: DOI 10.1109/TII.2017.2784561, IEEE Transactions on Industrial Informatics

$$\begin{cases} \dot{V}_i(t) = u_{vi}(t) \\ y_{vi}(t) = V_i(t) \end{cases} \quad (28)$$

We can design the distributed controller of reactive power control as

$$u_{vi}(t) = k_v e_{vi}(t) \quad (29)$$

Where k_v>0 and $e_{vi}(t)$ is defined as

$$e_{vi}(t) = \sum_{j\in N_i} [\hat{V}_j(t) - \hat{V}_i(t)] + d_i[V_{ref} - \hat{V}_i(t)] \quad (30)$$

where definition of the estimate is similar with that in (14).

Furthermore, in analogy with (15) and (16), we can define $\eta_{vi}(t)$ and the estimate error $\varepsilon_{vi}(t)$ of the voltage control, respectively, as the following to determine the event-triggered time

$$\eta_{vi}(t) = V_i(t) - V_{ref} \quad (31)$$

$$\varepsilon_{vi}(t) = V_i(t_k^{vi}) - V_i(t) \quad (32)$$

Theorem 3: Let G be connected and at least one agent can receive information from the leader node. Then the distributed controllers in (29) and (30) ensures global stability of the voltage dynamic system if the event-triggered time is defined by the following

$$t_k^{vi} = \inf\{t > t_{k-1}^{vi} \mid f_{vi}(t) = 0\} \quad (33)$$

where f_{vi}(t) can be defined as

$$f_{vi}(t) = \|\varepsilon_{vi}\|^2 - \frac{\alpha_v(1 - \beta_v \sum_{j\in N_i} a_{ij} - \beta_v d_i/2)}{\sum_{j\in N_i} a_{ij}/\beta_v + d_i/(2\beta_v)} \|e_{vi}\|^2 \quad (34)$$

where 0<α_v<1. Furthermore, there is

$$0 < \beta_v < \frac{1}{\sum_{j\in N_i} a_{ij} + d_i/2}, \forall i \quad (35)$$

Then combining (2), (4) and (28) yields

$$V_{ni}(t) = \int [u_{vi}(t) + D_{qi}(\omega_c q_i - \omega_c Q_i)]dt \quad (36)$$

The block diagram of the proposed secondary controllers is shown in Fig. 4. As seen, the DG*i* controller includes both DG*i* and DG*j* estimators and only the state values at the event-triggered time of DG*j* are communicated to the DG*j* estimator. Meanwhile, DG*i* transmits its state values to its neighbors only at its event-triggered time. Then secondary control inputs are generated by the outputs of estimators rather than the actual values of the corresponding variables. Therefore, in this way, the inter-agent communication is highly reduced and the scheme is more reliable.

C. Design Procedure

In this part, the design procedure of the proposed control strategy is summarized. According to the analysis above, the following steps can be derived:

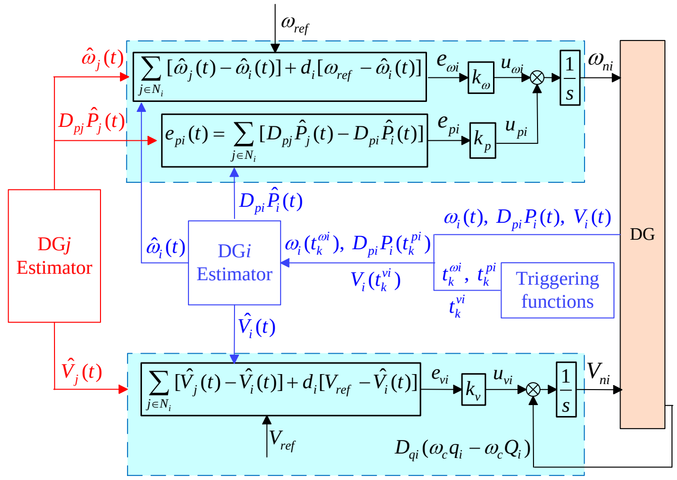

Fig. 4. Diagram of the proposed event-triggered based secondary controller.

1) Choose a proper communication whose corresponding graph is connected with at least one agent receiving information from the leader node.
2) Defining the local neighboring tracking errors as (13), (22) and (30). Thus the distributed controller can be constructed as (11), (21) and (29).
3) Determining the event triggered time instants according to Theorem 1, 2 and 3. To regulate the dynamic performance, all the constants in the controllers should be positive while satisfying the conditions in (19), (26) and (35).
4) Set the set-point values of the primary controllers as (27) and (36).

IV. Stability Analysis

In this section, we first use Lyapunov method to illustrate the stability of the proposed control strategy by proving the Theorems above, taking Theorem 1 as an example. Then we analysis the lower bound in the inter-event interval to show that the proposed strategy will not lead to infinite event-triggered instants in a finite time period, that is, no Zeno behavior [27], [28].

A. Proof of Theorem 1

Lemma 1 [29]: Let *G* is connected and at least one agent can receive information from the leader node. Then ***L***+***D*** is a symmetric positive definite matrix where ***D***=diag{d_i}.

In the following, we omit the subscript ω and abbreviate $x(t)$ to x for convenience. Combining (10), (11), (13)-(16) yields the stacked form as

$$\dot{\eta} = -k(\boldsymbol{L} + \boldsymbol{D})(\varepsilon + \eta) \quad (37)$$

where $\eta=[\eta_1, \eta_2, \ldots, \eta_N]^T$, $\varepsilon=[\varepsilon_1, \varepsilon_2, \ldots, \varepsilon_N]^T$. Similarly, there also is

$$e = -(\boldsymbol{L} + \boldsymbol{D})(\varepsilon + \eta) \quad (38)$$

where $e=[e_1, e_2, \ldots, e_N]^T$.

This article has been accepted for publication in a future issue of this journal, but has not been fully edited. Content may change prior to final publication. Citation information: DOI 10.1109/TII.2017.2784561, IEEE Transactions on Industrial Informatics

Considering the following Lyapunov function candidate

$$V=\frac{1}{2}\eta^{\mathrm{T}}(\boldsymbol{L}+\boldsymbol{D})\eta \tag{39}$$

Then the time derivative of (39) can be written as

$$\dot{V}=\eta^{\mathrm{T}}(\boldsymbol{L}+\boldsymbol{D})\dot{\eta} \tag{40}$$

Combining with the dynamic of η in (37) yields

$$\dot{V}=-k\eta^{\mathrm{T}}(\boldsymbol{L}+\boldsymbol{D})^2(\varepsilon+\eta) \tag{41}$$

On the other hand, Lemma 1 implies $\boldsymbol{L}$+$\boldsymbol{D}$ is reversible, then place (38) into the upper equation in (41) yields

$$\dot{V}=-ke^{\mathrm{T}}(\boldsymbol{L}+\boldsymbol{D})\varepsilon-ke^{\mathrm{T}}e=-ke^{\mathrm{T}}(\boldsymbol{L}+\boldsymbol{D})\varepsilon-k\,||\,e\,||^2 \tag{42}$$

We can expand the upper equation in (42) as

$$\dot{V}=-k\sum_{i=1}^{N}||\,e_i\,||^2-k\sum_{i=1}^{N}\sum_{j\in N_i}e_i\varepsilon_i-k\sum_{i=1}^{N}d_ie_i\varepsilon_i$$

$$+k\sum_{i=1}^{N}\sum_{j\in N_i}e_i\varepsilon_j \tag{43}$$

Note that

$$x^{\mathrm{T}}y\le\frac{\beta}{2}||\,x\,||^2+\frac{1}{2\beta}||\,y\,||^2,\ \beta>0 \tag{44}$$

the upper equation in (43) can be upper bounded by

$$\dot{V}\le-k\sum_{i=1}^{N}||\,e_i\,||^2+k\sum_{i=1}^{N}\sum_{j\in N_i}\beta\,||\,e_i\,||^2+k\sum_{i=1}^{N}\sum_{j\in N_i}\frac{1}{2\beta}||\,\varepsilon_i\,||^2$$

$$+k\sum_{i=1}^{N}d_i\frac{\beta}{2}||\,e_i\,||^2+k\sum_{i=1}^{N}d_i\frac{1}{2\beta}||\,\varepsilon_i\,||^2+k\sum_{i=1}^{N}\sum_{j\in N_i}\frac{1}{2\beta}||\,\varepsilon_j\,||^2 \tag{45}$$

Considering that G is undirected, we have

$$\sum_{i=1}^{N}\sum_{j\in N_i}||\,\varepsilon_j\,||^2=\sum_{i=1}^{N}\sum_{j\in N_i}||\,\varepsilon_i\,||^2 \tag{46}$$

Placing (46) into (45) yields

$$\dot{V}\le k\sum_{i=1}^{N}(\beta\sum_{j\in N_i}a_{ij}+d_i\frac{\beta}{2}-1)\,||\,e_i\,||^2$$

$$+k\sum_{i=1}^{N}(\frac{1}{\beta}\sum_{j\in N_i}a_{ij}+\frac{d_i}{2\beta})\,||\,\varepsilon_i\,||^2 \tag{47}$$

Considering the triggering function defined in (18) and Fig. 3, the time derivative in (47) can be upper bounded by

$$\dot{V}\le k\sum_{i=1}^{N}(\alpha-1)(1-\beta\sum_{j\in N_i}a_{ij}-d_i\frac{\beta}{2})\,||\,e_i\,||^2 \tag{48}$$

Combining (48) with (19) yields

$$\dot{V}\le 0 \tag{49}$$

Thus the disagreement η is globally stable. This completes the proof.

B. Minimal Inter-event interval

Theorem 4: Let G is connected and at least one agent can receive information from the leader node. Considering the system in (10) with the distributed controller in (11) and (13), the triggering function defined in (18) ensures that there exists at least one agent $v_h\in V(G)$ such that the inter-event interval is lower bounded by a positive constant τ

Proof: Investigating the time derivative as following

$$\frac{d}{dt}\frac{||\,\varepsilon\,||}{||\,e\,||}\le\frac{||\,\dot{\varepsilon}\,||}{||\,e\,||}+\frac{||\,\varepsilon\,||||\,\dot{e}\,||}{||\,e\,||^2} \tag{50}$$

From (13) to (16), there is

$$\frac{d}{dt}\frac{||\,\varepsilon\,||}{||\,e\,||}\le k\frac{||\,\boldsymbol{L}+\boldsymbol{D}\,||\,(||\,\varepsilon\,||+||\,\eta\,||)}{||\,e\,||} \tag{51}$$

Noting $\boldsymbol{L}$+$\boldsymbol{D}$ is reversible combing (51) with (38) yields

$$\frac{d}{dt}\frac{||\,\varepsilon\,||}{||\,e\,||}\le\gamma\frac{||\,\varepsilon\,||}{||\,e\,||}+\gamma \tag{52}$$

where

$$\gamma=\max\{2k\,||\,L+D\,||,\ k\} \tag{53}$$

Thus $||\varepsilon||/||e||$ is upper bounded by

$$\frac{||\,\varepsilon\,||}{||\,e\,||}\le\Phi(t,\ \Phi_0) \tag{54}$$

where $\Phi(t,\ \Phi_0)$ is the solution of the following differential equations as

$$\begin{cases}\dot{\Phi}=\gamma\Phi+\gamma\\ \Phi(0,\Phi_0)=\Phi_0\end{cases} \tag{55}$$

Further, there is

$$\Phi(\tau,0)=\exp(\gamma\tau)-1 \tag{56}$$

On the other hand, defining that

$$h=\arg\max_{v_i\in V(D)}||\,e_i\,|| \tag{57}$$

Thus the following inequality holds

$$\frac{||\,\varepsilon_h\,||}{||\,e_h\,||}\le\frac{||\,\varepsilon\,||}{||\,e_h\,||}\le\frac{N\,||\,\varepsilon\,||}{||\,e\,||} \tag{58}$$

According to (58) and the definition of the triggering function in (18), the following formula is obtained

$$\sqrt{\frac{\alpha(1-\beta\sum_{j\in N_i}a_{ij}-\beta d_i/2)}{\sum_{j\in N_i}a_{ij}/\beta+d_i/(2\beta)}}\le N[\exp(\gamma\tau)-1] \tag{59}$$

Thus the minimum inter-event interval of agent$h$ is lower

This article has been accepted for publication in a future issue of this journal, but has not been fully edited. Content may change prior to final publication. Citation information: DOI 10.1109/TII.2017.2784561, IEEE Transactions on Industrial Informatics

bounded by τ, i.e.,

$$\tau \geq \frac{1}{\gamma}\ln\left[\frac{1}{N}\sqrt{\frac{\alpha(1-\beta\sum_{j\in N_i} a_{ij} - \beta d_i/2)}{\sum_{j\in N_i} a_{ij}/\beta + d_i/(2\beta)}} + 1\right] \qquad (60)$$

This completes the proof.

V. Simulation Results

In order to verify the effectiveness of the proposed distributed secondary control strategies, a 380V/50Hz islanded microgrid test system including four DGs and two Loads, shown in Fig. 5, is built in PSCAD/EMTDC. The specification of the test system is listed in Table I. It should be noted that, as seen in Table I, the parameters of DGs are not necessarily identical. In general, set-points of secondary level can choose as their nominal values. The communication graph chosen in the simulation is also shown in Fig. 5. As seen, it satisfies the condition that being connected. In addition, only DG1 can access to the references. Furthermore, we suppose a 5ms interval to denote the minimal communication period of the actual communication network.

A. Performance of the proposed secondary control

At the beginning, only the primary control is activated and all the four DGs supply for the loads. Then the proposed secondary controllers are started at t=2s. The results are shown in Fig. 6. As seen, the primary control guarantees that all DGs share the active power according to their droop coefficients. However, all output voltages and the frequencies deviate from the nominal values due to the droop characteristics. Then after t=2s, they can gradually restore to their nominal values, i.e., V_{ref}=1p.u. and f_{ref}=50Hz, subjected to the proposed secondary control function. Meanwhile, the accurate active power sharing can be guaranteed in the steady state. Fig. 6 also shows that the output active powers increase after the secondary control being in action. This is duo to the load characteristics. At t=7s, Load 2 is disconnected from the system. Then, at t=12s, Load 2 is connected to the system again. As seen, the proposed secondary control strategy can keep the voltage and frequency of DGs at the nominal values while keeping accurate active power sharing response to both load connection and disconnection.

Fig. 7 shows the dynamics of the proposed controllers under different gains taking DG1 as an example. It can be seen that when the gains increase to two times of their original values, the regulation time decrease to 50%, which means that larger gains increase reaction speed of the system. However, this requires larger sampling rate. In the application of microgrid, the time scale of secondary control is about several seconds [5], [34]. Therefore, the gain values used in the paper is enough for the secondary control of microgrid.

B. Plug-and-play verification

This part tests the plug-and-play ability of the proposed control strategy, and the results are shown in Fig. 8. In the

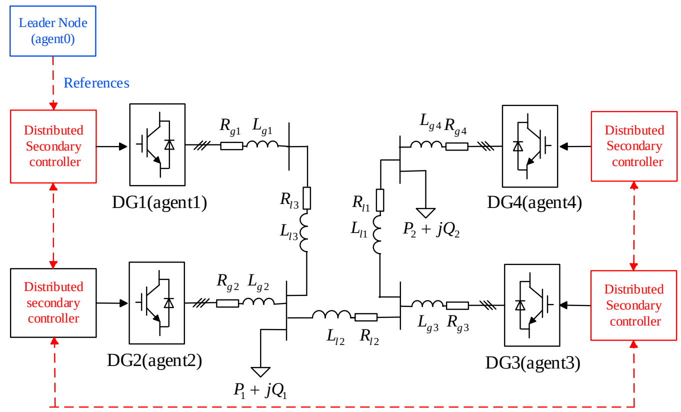

Fig. 5. Islanded microgrid test system.

TABLE I
Parameters of islanded microgrid and its control system

	DG1		DG2		DG3		DG4	
DGs	R_{g1}	0.03Ω	R_{g2}	0.03Ω	R_{g3}	0.03Ω	R_{g4}	0.03Ω
	L_{g1}	0.35mH	L_{g2}	0.35mH	L_{g3}	0.35mH	L_{g4}	0.35mH
	D_{p1}	12.5e-5	D_{p2}	12.5e-5	D_{p3}	9.4e-5	D_{p4}	9.4e-5
	D_{q1}	1.5e-3	D_{q2}	1.5e-3	D_{q3}	1.3e-3	D_{q4}	1.3e-3
lines	Line1		Line2		Line3			
	R_{g1}	0.23Ω	R_{g2}	0.35Ω	R_{g3}	0.23Ω		
	L_{g1}	0.318mH	L_{g2}	1.847mH	L_{g3}	0.318mH		
loads	Load1		Load2					
	P_1	45.9kW	P_3	36kW				
	Q_1	22.8kVar	Q_3	36kVar				
gain	k_v	6						
	k_ω	4						
	k_p	4						

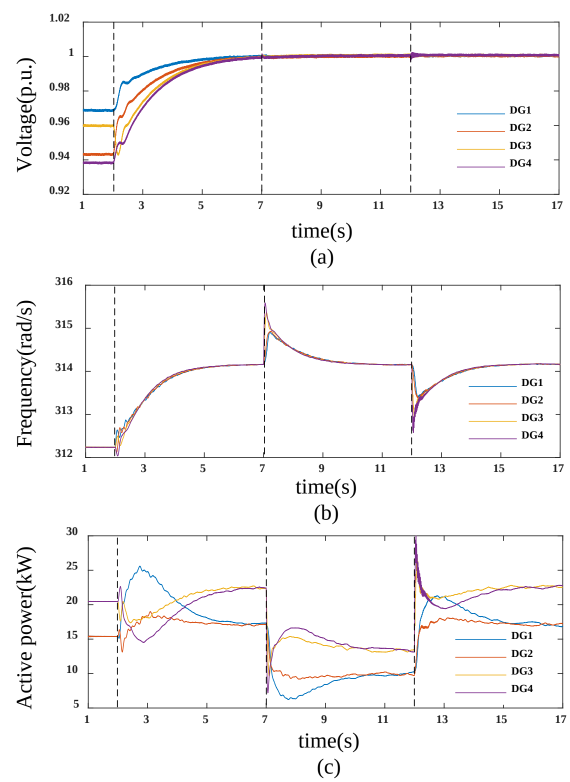

Fig. 6. Outputs of the test islanded microgrid.

simulation, DG4 is disconnected from the network at t=8s and reconnected again at t=13s. As seen in Fig. 5, the graph is still connected with agent1 receiving information from the leader

This article has been accepted for publication in a future issue of this journal, but has not been fully edited. Content may change prior to final publication. Citation information: DOI 10.1109/TII.2017.2784561, IEEE Transactions on Industrial Informatics

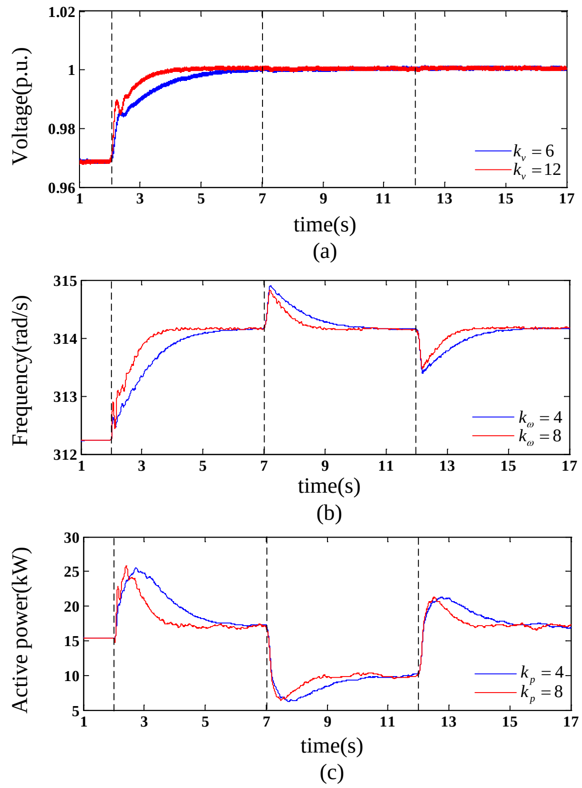

Fig. 7. Simulation results under different control gains.

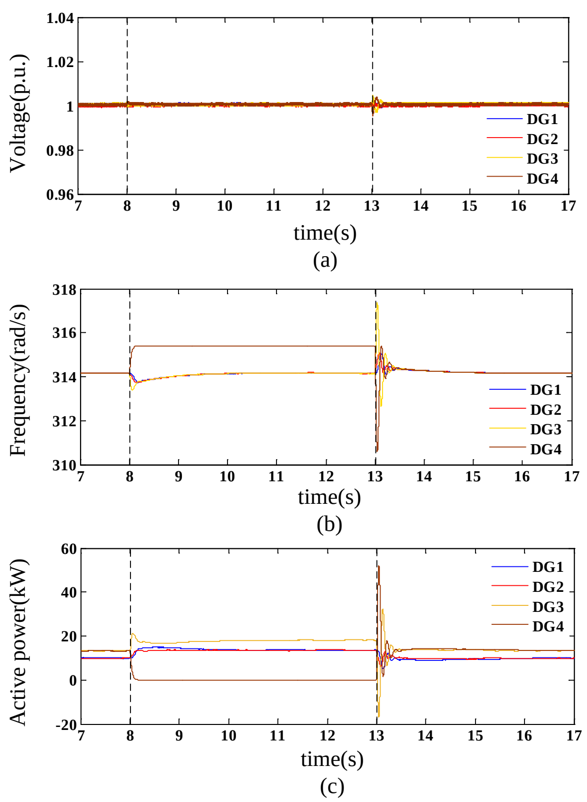

Fig. 8. Performance of plug and play.

node when DG4 is disconnected. Therefore, targets of secondary control can still be achieved by DG1, DG2 and DG3. Fig. 8 also shows that the system endures serious oscillation when DG4 is reconnected. This is because no pre-synchronization is implemented. However, the transient frequency is kept in ±0.6Hz and system can still keep stable even in this situation.

C. Comparison with the traditional way

The relevant results about microgrid secondary control are usually based on periodic states feedback control [7]-[11], [13]. Therefore, a comparison between the proposed event-triggered control and the traditional control, using same control gains, is made in this paper. The simulation results, taking DG1 as an example, are shown in Fig. 9. As seen, the proposed event-triggered way can have a similar settling time with that of the traditional control way. This further proves the effectiveness of the proposed control strategy. However, the event-triggered method exhibits a little more oscillation. In addition, due to the states updating at the event-triggered time, sawtooth waves can be observed in the event-triggered way. Furthermore, Fig. 10 shows system dynamics with respect to load variation. At t=9s, Load 2 is disconnected from the system. As seen, voltage of DG1 is hardly influenced because it's far away from Load2 as shown in Fig. 5. And the proposed strategy can keep the voltage and frequency at their nominal values after the transient. Also output power decrease due to load shedding.

To illustrate the communication mechanism of the proposed control strategy and compare communication burden with the traditional approach， Fig. 11 shows, taking DG1 as an example, the event time instants of the distributed voltage, frequency and active power controllers. It should be noted that， for traditional way, periodic communication with a 5ms interval is considered. In addition, the results about communication burden in the time frame 2s-6s are depicted in Table II. From Fig. 11 and Table II, it is concluded that the proposed distributed control strategy can highly reduce communication burden between DGs while restoring voltage and frequency to the nominal values.

D. Performance under communication delays

In this section, the performance of the proposed control strategy, taking DG1 as an example, is investigated under different communication delays. It is observed from Fig. 12 that the response of the system become more oscillatory as the communication delays increase. This is because that the triggering functions are designed by Lyapunov method and the communication delays will decrease the stability margin. However, the system is still table according to the simulation results. It is worth noting that the communication delays are usually in the order of milliseconds or tens of milliseconds [5]. Thus, the proposed control strategy can meet the requirments in practice.

VI. Conclusion

The distributed cooperative secondary restoration problem of the islanded microgrid using event-triggered control strategy is addressed in this paper.

1) Both of voltage and frequency can be restored to their nominal values while keeping the active power sharing

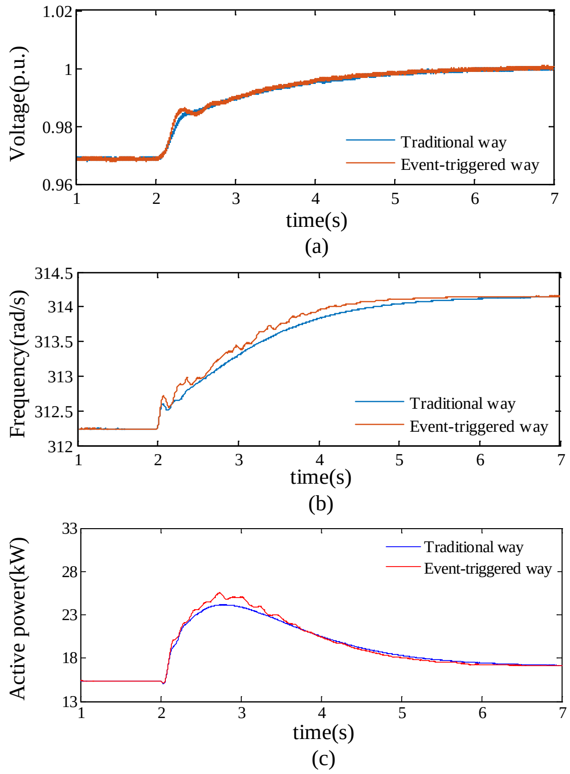

Fig. 9. Comparison between the proposed control way and the traditional way.

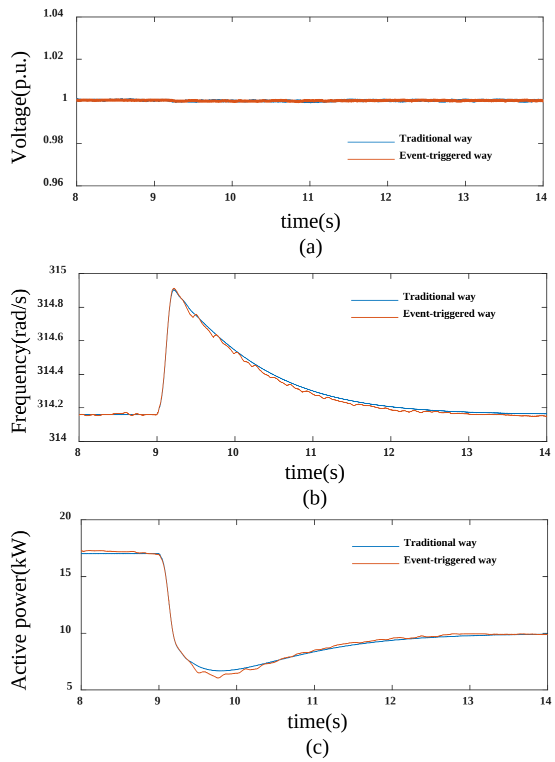

Fig. 10. Comparison with respect to load variation between the proposed control way and the traditional way.

accurary

2) Communication burden between secondary controllers of the DGs is highly reduced.
3) The defined event-triggered time based on decentralized event triggering functions for every DGs

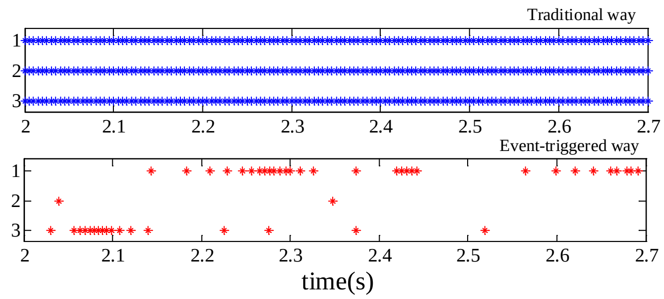

Fig. 11. The trigger event instants for DG1 (1: voltage controller, 2: frequency controller and 3: active power controller).

TABLE II
Communication of secondary control

DGs	Controllers	Number of communication events		Average intervals between two contiguous events	
		Traditional way	Event-triggered way	Traditional way	Event-triggered way
DG1	Voltage	799	223	5ms	18ms
	Frequency	799	9	5ms	400ms
	Active power	799	21	5ms	182ms
DG2	Voltage	799	221	5ms	18ms
	Frequency	799	329	5ms	12ms
	Active power	799	167	5ms	24ms
DG3	Voltage	799	200	5ms	20ms
	Frequency	799	371	5ms	11ms
	Active power	799	78	5ms	51ms
DG4	Voltage	799	49	5ms	80ms
	Frequency	799	334	5ms	12ms
	Active power	799	36	5ms	108ms

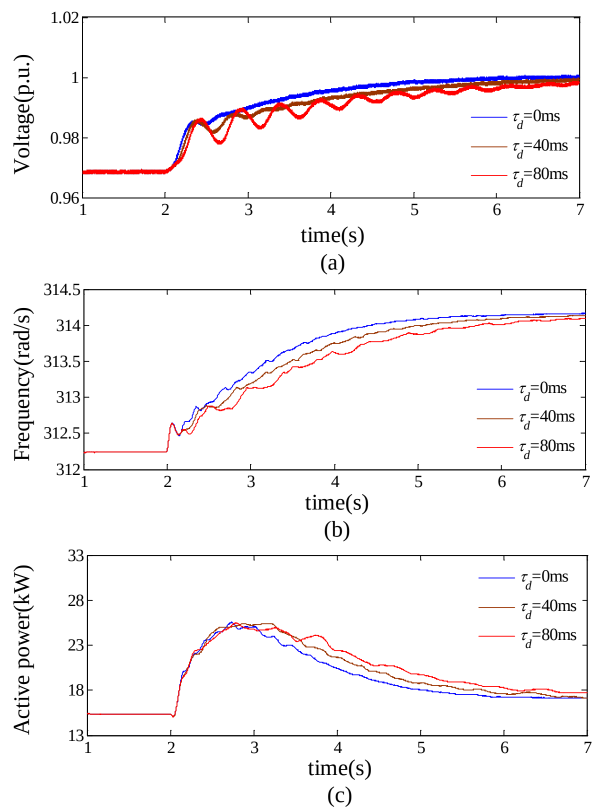

Fig. 12. Performance under different communication delays.

can keep the stability of the distributed control system while keeping away Zeno behavior.

Furthermore, impact of packet loss on performance of event-triggered control will be studied in the future because the microgrid control may be implemented on a network with high packet-drop rate. Meanwhile, advanced control methods such as finite-time control can be investigated combining with the event-triggered communication to increase reaction speed of the secondary controllers.

VII. References

[1] J. M. Guerrero, M. Chandorkar, T.-L. Lee, and P. C. Loh, "Advanced Control Architectures for Intelligent Microgrids-Part I: Decentralized and Hierarchical Control," *IEEE Trans. Ind. Electron.*, vol. 60, no. 4, pp. 1254–1262, Apr. 2013.

[2] A. Bidram, A. Davoudi, and F. L. Lewis, "A multiobjective distributed control framework for islanded AC microgrids," *IEEE Trans. Ind. Informatics*, vol. 10, no. 3, pp. 1785–1798, Aug. 2014.

[3] J. M. Guerrero, J. C. Vasquez, J. Matas, L. G. de Vicuna, and M. Castilla, "Hierarchical Control of Droop-Controlled AC and DC Microgrids-A General Approach Toward Standardization," IEEE Trans. Ind. Electron., vol. 58, no. 1, pp. 158–172, Jan. 2011.

[4] A. Bidram and A. Davoudi, "Hierarchical Structure of Microgrids Control System," IEEE Trans. Smart Grid, vol. 3, no. 4, pp. 1963–1976, Dec. 2012.

[5] C. Ahumada, R. Cardenas, D. Saez, and J. M. Guerrero, "Secondary Control Strategies for Frequency Restoration in Islanded Microgrids With Consideration of Communication Delays," IEEE Trans. Smart Grid, vol. 7, no. 3, pp. 1430–1441, May 2016.

[6] D. E. Olivares et al., "Trends in Microgrid Control," IEEE Trans. Smart Grid, vol. 5, no. 4, pp. 1905–1919, Jul. 2014.

[7] F. L. Lewis, Z. Qu, A. Davoudi, and A. Bidram, "Secondary control of microgrids based on distributed cooperative control of multi-agent systems," IET Gener. Transm. Distrib., vol. 7, no. 8, pp. 822–831, Aug. 2013.

[8] A. Bidram, A. Davoudi, F. L. Lewis, and J. M. Guerrero, "Distributed Cooperative Secondary Control of Microgrids Using Feedback Linearization," IEEE Trans. Power Syst., vol. 28, no. 3, pp. 3462–3470, Aug. 2013.

[9] F. Guo, C. Wen, J. Mao, and Y.-D. Song, "Distributed Secondary Voltage and Frequency Restoration Control of Droop-Controlled Inverter-Based Microgrids," IEEE Trans. Ind. Electron., vol. 62, no. 7, pp. 4355–4364, Jul. 2015.

[10] S. Zuo, A. Davoudi, Y. Song, and F. L. Lewis, "Distributed Finite-Time Voltage and Frequency Restoration in Islanded AC Microgrids," IEEE Trans. Ind. Electron., vol. 63, no. 10, pp. 5988–5997, Oct. 2016.

[11] L.-Y. Lu and C.-C. Chu, "Consensus-Based Secondary Frequency and Voltage Droop Control of Virtual Synchronous Generators for Isolated AC Micro-Grids," IEEE J. Emerg. Sel. Top. Circuits Syst., vol. 5, no. 3, pp. 443–455, Sep. 2015.

[12] Yuan Fang, Guoqiang Hu, and M. Egerstedt, "Distributed reactive power sharing control for microgrids with event-triggered communication," IEEE Trans. Contr. Syst. Technology, vol. 25, no. 1, pp. 118–128, Jan. 2017.

[13] Xiaoqing Lu, Xinghuo Yu, Jingang Lai, J. M. Guerrero, and Hong Zhou, "Distributed secondary voltage and frequency control for islanded microgrids with uncertain communication links," IEEE Trans. Ind. Informatics, vol. 13, no. 2, pp. 448–460, Apr. 2017.

[14] M. Tahir and S. K. Mazumder, "Self-triggered communication enabled control of distributed generation in microgrids," IEEE Trans. Ind. Informatics, vol. 11, no. 2, pp. 441–449, Apr. 2015.

[15] Renke Han, N. L. D. Aldana, Lexuan Meng, J. M. Guerrero, and Qiuye Sun, "Droop-free distributed control with event-triggered communication in DC micro-grid," 2017 IEEE Applied Power Electronics Conference and Exposition, pp. 1160–1166, 2017.

[16] S. D'Arco, J. A. Suul, and O. B. Fosso, "A Virtual Synchronous Machine implementation for distributed control of power converters in SmartGrids," Electr. Power Syst. Res., vol. 122, pp. 180–197, May 2015.

[17] Fang Gao and M. R. Iravani, "A Control Strategy for a Distributed Generation Unit in Grid-Connected and Autonomous Modes of Operation," IEEE Trans. Power Deliv., vol. 23, no. 2, pp. 850–859, Apr. 2008.

[18] H. Wu et al., "Small-Signal Modeling and Parameters Design for Virtual Synchronous Generators," IEEE Trans. Ind. Electron., vol. 63, no. 7, pp. 4292–4303, Jul. 2016.

[19] Y. Mohamed and E. F. El-Saadany, "Adaptive Decentralized Droop Controller to Preserve Power Sharing Stability of Paralleled Inverters in Distributed Generation Microgrids," IEEE Trans. Power Electron., vol. 23, no. 6, pp. 2806–2816, Nov. 2008.

[20] R. Kabiri, D. G. Holmes, and B. P. McGrath, "Control of Active and Reactive Power Ripple to Mitigate Unbalanced Grid Voltages," IEEE Trans. Ind. Appl., vol. 52, no. 2, pp. 1660–1668, Mar. 2016.

[21] Youfeng Su and Jie Huang, "Cooperative Output Regulation of Linear Multi-Agent Systems," IEEE Trans. Automat. Contr., vol. 57, no. 4, pp. 1062–1066, Apr. 2012.

[22] F. Guo, C. Wen, J. Mao, J. Chen, and Y.-D. Song, "Distributed Cooperative Secondary Control for Voltage Unbalance Compensation in an Islanded Microgrid," IEEE Trans. Ind. Informatics, vol. 11, no. 5, pp. 1078–1088, Oct. 2015.

[23] Hongwei Zhang, F. L. Lewis, and A. Das, "Optimal Design for Synchronization of Cooperative Systems: State Feedback, Observer and Output Feedback," IEEE Trans. Automat. Contr., vol. 56, no. 8, pp. 1948–1952, Aug. 2011.

[24] D. Xie, D. Yuan, J. Lu, and Y. Zhang, "Consensus control of second-order leader-follower multi-agent systems with event-triggered strategy," Trans. Inst. Meas. Control, vol. 35, no. 4, pp. 426–436, 2013.

[25] Y. Wu, X. Meng, L. Xie, R. Lu, H. Su, and Z.-G. Wu, "An input-based triggering approach to leader-following problems," Automatica, vol. 75, pp. 221–228, Jan. 2017.

[26] Xianming Zhang, Qinglong Han, and Xinghuo Yu, "Survey on recent advances in networked control systems," IEEE Trans. Ind. Informatics, vol. 12, no. 5, pp. 1740–1752, Oct. 2016.

[27] C. Nowzari and J. Cortes, "Zeno-free, distributed event-triggered communication and control for multi-agent average consensus," in 2014 American Control Conference, 2014, pp. 2148–2153.

[28] E. Garcia, Y. Cao, and D. W. Casbeer, "Decentralized event-triggered consensus with general linear dynamics," Automatica, vol. 50, no. 10, pp. 2633–2640, Oct. 2014.

[29] Zhongkui Li, Zhisheng Duan, Guanrong Chen, and Lin Huang, "Consensus of Multiagent Systems and Synchronization of Complex Networks: A Unified Viewpoint," IEEE Trans. Circuits Syst. I Regul. Pap., vol. 57, no. 1, pp. 213–224, Jan. 2010.

[30] F. Cheng, F. Hao, "Event-triggered control for linear descriptor systems," Circuits Syst. Signal Process, vol. 32, no. 3, pp. 1065-1079, Jun. 2013.

[31] M. S. Mahmoud, M. S. U. Rahman, "Event triggered of microgrid control with communication and control optimization," J. Franklin Institute, vol. 353, no. 16, pp. 4114-4132, Aug. 2016.

[32] Y. Han, H. Li, P. Shen, E. A. A. Coelho, J. M. Guerrero, "Review of active and reactive power sharing strategies in hierarchical cotrolled microgrids," IEEE Trans. Power Electron., vol. 32, no. 3, pp. 2427-2451.

[33] H. Xin, R. Zhao, L. Zhang, Z. Wang, K. P. Wong, W. Wei, "A decentralized hierarchical control structure and self-optimizing control strategy for F-P type DGs in islanded microgrids," IEEE Trans. Smart Grid, vol. 7, no. 1, pp. 3-5.

[34] S. Liu, X. Wang, P. X. Liu, "Impact of communication delays on secondary frequency control in an islanded microgrid," IEEE Trans. Ind. Electron., vol. 62, no. 4, pp. 2021-2031.

[35] M. H. Amini, K. G. Boroojeni, T. Dragičević, A. Nejadpak, S. S. Iyengar, and F. Blaabjerg, "A comprehensive cloud-based real-time simulation framework for oblivious power routing in clusters of DC microgrids," 2017 IEEE Second International Conference on DC Microgrids (ICDCM), pp. 270–273, 2017.